

PROBING THE SHAPE OF THE GALACTIC HALO WITH HYPER-VELOCITY STARS

OLEG Y. GNEDIN¹, ANDREW GOULD¹, JORDI MIRALDA-ESCUDE¹, ANDREW R. ZENTNER²

Draft version July 11, 2018

ABSTRACT

Precise proper motion measurements ($\sigma_\mu \sim 10 \mu\text{as yr}^{-1}$) of the recently discovered hyper-velocity star (HVS) SDSS J090745.0+024507 would yield significant constraints on the axis ratios and orientation of a triaxial model for the Galactic halo. Triaxiality of dark matter halos is predicted by Cold Dark Matter models of galaxy formation and may be used to probe the nature of dark matter. However, unless the distance to this star is determined to better than 10%, these constraints suffer from one-dimensional degeneracies, which we quantify. We show how proper motion measurements of several HVSs could simultaneously resolve the distance degeneracies of all such stars and produce a detailed picture of the triaxial halo. Additional HVSs may be found from radial velocity surveys or from parallax/proper-motion data derived from GAIA. High-precision proper-motion measurements of these stars using the *Space Interferometry Mission (SIM PlanetQuest)* would substantially tighten the constraints they yield on the Galactic potential.

Subject headings: cosmology: theory — dark matter : halos: structure — galaxies: formation

1. INTRODUCTION

In the course of a spectroscopic survey of candidate faint blue horizontal-branch stars found in the Sloan Digital Sky Survey, Brown et al. (2005) have discovered a star with the heliocentric radial velocity $v_{\text{obs}} = +853 \pm 12 \text{ km s}^{-1}$ at the Galactic coordinates $b = 31.3319^\circ$, $l = 227.3353^\circ$. The velocity of this star, SDSS J090745.0+024507 (hereafter called “the hyper-velocity star”, or HVS), is more than twice the escape speed from the Galaxy at the star’s present location. Corrected for the solar motion relative to the local standard of rest (LSR; Dehnen & Binney 1998), the line-of-sight (los) LSR velocity is $v_{\text{los}} = 848 \text{ km s}^{-1}$. The distance of the HVS from Earth is presently uncertain due to an ambiguity in its spectral classification. If it is a main sequence B9 star, its heliocentric distance is $d \approx 70 \text{ kpc}$; if it is a blue horizontal branch star, then $d \approx 40 \text{ kpc}$. A higher S/N spectrum from a large ground-based telescope should determine the spectral type of this star.

As discussed by Brown et al. (2005), the velocity of the HVS greatly exceeds that plausible for a runaway star ejected from a binary in which one component has undergone a supernova explosion. The only known mechanism for a star to obtain such an extreme velocity is ejection from the deep potential of the massive black hole at the Galactic center, as a result of scattering with another star or tidal breakup of a binary (Hills 1988; Yu & Tremaine 2003). Only extremely close to the massive black hole, at $r \lesssim 0.01 \text{ pc}$, can stars attain the required speeds $v \approx (2GM_{\text{bh}}/r)^{1/2} \gtrsim 1000 \text{ km s}^{-1}$.

A precise measurement of the three-dimensional motion of this HVS can probe the shape of the mass distribution of the Galactic halo in a way that is independent of any other technique attempted so far. The expected trajectory of the HVS in the Galaxy is almost a straight

line, owing to its extremely high velocity. However, assuming its origin at the Galactic center, the direction of the HVS’s present velocity should deviate slightly from being precisely radial due to departures from spherical symmetry of the Galactic potential.

The main sources of such asymmetry are the flattened disk and the (possibly) triaxial dark matter halo. Several estimates of the halo shape based on observations of tidal debris associated with the Sagittarius dwarf galaxy indicate that it is close to spherical (e.g. Ibata et al. 2001; Majewski et al. 2003; Johnston et al. 2005), although Helmi (2004a) argues that minor-to-major axis ratios as low as 0.6 for isodensity contours cannot be ruled out for a prolate halo oriented with its major axis along the rotation axis of the disk. While cosmological N-body simulations based on Cold Dark Matter models typically produce prolate halos with density axis ratios in the range 0.5 – 0.8 (e.g. Jing & Suto 2002; Bullock 2002), gasdynamics simulations indicate that the effects of gas cooling and dissipation tend to make the halos rounder (Kazantzidis et al. 2004). Whether the predictions of gasdynamics simulations agree with the observations of tidal streams still remains to be seen.

Measuring the proper motions of the HVS and reconstructing its three-dimensional velocity will provide useful constraints on the shape and orientation of the Galactic dark matter halo, as we discuss below. Independent observational constraints of halo shapes are important for testing structure formation models as well as probing the nature of dark matter.

2. ORBITS OF THE HYPER-VELOCITY STAR

In order to evaluate the deviation of the HVS orbit from a straight line, we have calculated a family of orbits of the HVS consistent with its position in the sky (Galactic coordinates l and b), the assumed distance from Earth (d), and the observed line-of-sight velocity, v_{los} . All orbits start at the origin $r = 0$ with some initial ejection velocity \mathbf{v}_i , which is then adjusted until the orbit reproduces the four observables.

We approximate the Galactic potential by the sum of

¹ Department of Astronomy, The Ohio State University, 140 W 18th Ave., Columbus, OH 43210; ognedin@astronomy.ohio-state.edu

² Kavli Institute for Cosmological Physics and Department of Astronomy and Astrophysics, The University of Chicago, Chicago, IL 60637

three components: spherical bulge, axisymmetric disk, and triaxial dark matter halo, with parameters that are consistent with the current mass model of the Galaxy by Klypin et al. (2002). The bulge potential is given by the Hernquist (1990) model:

$$\Phi_b(r) = -\frac{GM_b}{r + a_b}, \quad (1)$$

with mass $M_b = 10^{10} M_\odot$ and core radius $a_b = 0.6$ kpc. The disk potential is given by the analytical Miyamoto & Nagai (1975) model:

$$\Phi_d(R, z) = -\frac{GM_d}{\sqrt{R^2 + (a_d + (z^2 + b_d^2)^{1/2})^2}} \quad (2)$$

with mass $M_d = 4 \times 10^{10} M_\odot$, scale length $a_d = 5$ kpc, and scale height $b_d = 0.3$ kpc. The halo potential is derived from a generalized triaxial density distribution of the NFW model (Navarro et al. 1997), which provides a good fit to halo profiles found in cosmological N-body simulations (Jing & Suto 2002):

$$\rho_h(\tilde{r}) = \frac{M_h}{4\pi\tilde{r}(\tilde{r} + r_s)^2}, \quad (3)$$

with mass $M_h = 10^{12} M_\odot$ and scale radius $r_s = 20$ kpc. We generalize the halo profile as a function of the triaxial radius \tilde{r} to allow for three independent scale lengths:

$$\tilde{r}^2 \equiv (x/q_1)^2 + (y/q_2)^2 + (z/q_3)^2. \quad (4)$$

We explore the full range of the axis ratios consistent with current observational constraints, $0.5 \leq q_i \leq 1$, to investigate the maximum effect of halo triaxiality on the expected proper motions of the HVS. Specifically, we calculate three sets of models with the halo major axis aligned with each of the three coordinate axes while varying the other two axis ratios from 0.5 to 1 with a step 0.05. For simplicity we assume that the axis ratios are constant as a function of radius, an assumption that is supported by the results of cosmological N-body simulations (e.g. Jing & Suto 2002). In practice, the motion of the HVS probes the halo shape in the range of radii between 20 and 80 kpc (see Fig. 2). We also do not include the effect of adiabatic contraction of the halo in response to the central concentration of baryons (Blumenthal et al. 1986; Ryden & Gunn 1987; Gnedin et al. 2004) since this effect is likely to be small at large radii, $r \gtrsim r_s$.

The triaxial halo potential is obtained by numerical integration over thin triaxial shells, or homeoids (e.g. Binney & Tremaine 1987, Chapter 2.3). Interior to the shell the potential is constant, while isopotential surfaces exterior to the shell are confocal ellipsoids labeled by the parameter τ :

$$\text{const} = m^2 \equiv q_1^2 \sum_i \frac{x_i^2}{q_i^2 + \tau}. \quad (5)$$

The exterior potential due to each such shell m is proportional to $\psi(\infty) - \psi(m[\tau])$, where

$$\psi(m) \equiv \int_0^{m^2} \rho(m^2) dm^2 = \frac{M_h}{2\pi r^2} \frac{m}{m + r_s}, \quad (6)$$

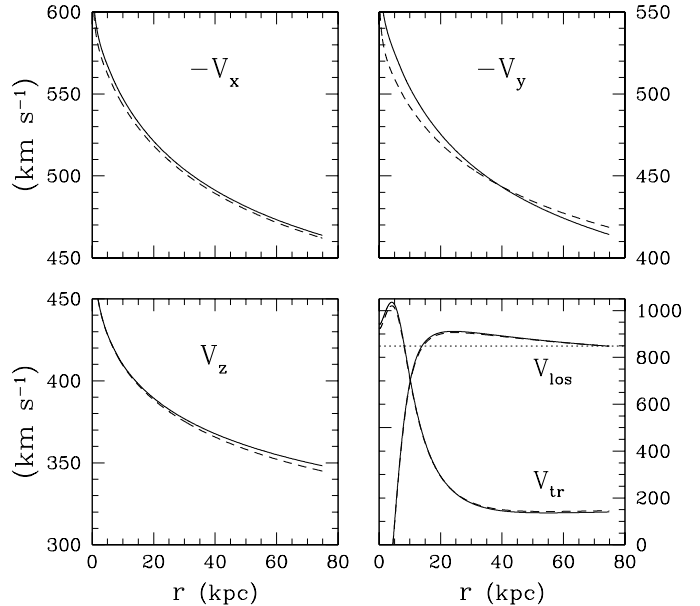


FIG. 1.— Deceleration of the HVS as a function of distance to the Galactic center. Three velocity components in the Galactocentric frame are shown for the cases of a spherical halo (dashed lines) and a triaxial halo (solid lines). The axis ratios of the triaxial model are $q_1/q_3 = 0.9$, $q_2/q_3 = 0.7$, and the assumed current distance from Earth is $d = 70$ kpc. The bottom right panel shows the line-of-sight velocity as seen from Earth and the absolute value of the transverse velocity. The observed los velocity is shown by a horizontal dotted line.

and the second equality is for the density profile given by equation (3). The total potential is the integral over all shells,

$$\Phi_h(x, y, z) = -\frac{GM_h}{2} \frac{q_2 q_3}{q_1} \times \int_0^\infty \frac{d\tau}{(m + r_s) \sqrt{(q_1^2 + \tau)(q_2^2 + \tau)(q_3^2 + \tau)}}. \quad (7)$$

We have tabulated the integral in equation (7), as well as the corresponding integrals for the force components, on a three-dimensional grid of coordinates (x, y, z) and interpolated the tables for orbit calculation.

With our definition of the triaxial profile (eq. [3]) the halo mass enclosed within a given spherical radius R_{vir} depends on the axis ratios. The more triaxial halos have less enclosed mass. On the other hand, the measured mass of the Galaxy, inferred from the radial velocities of distant satellites and globular clusters, is in principle independent of halo triaxiality. In order to fix this discrepancy, we have renormalized the mass M_h for triaxial halo cases such that the mass within a spherical virial radius $R_{\text{vir}} = 12 r_s$ (see Klypin et al. 2002) is the same for all models and equals $10^{12} M_\odot$.

Figure 1 illustrates the deceleration of the HVS on its way from the Galactic center for both a spherical halo model and a triaxial halo model. A typical ejection velocity is 900 km s^{-1} in the Galactocentric frame, which is reduced to 700 km s^{-1} at the present position. The line-of-sight direction varies rapidly at small distances $r < 20$ kpc, when the HVS is relatively close to Earth,

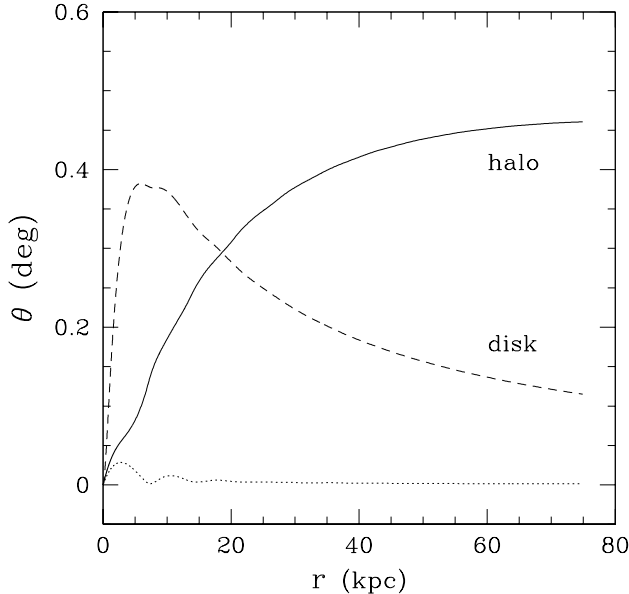


FIG. 2.— Angle between the radius vector and the velocity vector of the HVS in the Galactocentric frame vs the distance to the Galactic center, for the orbits shown on Fig. 1. Solid line shows the apparent deflection of the orbit from a straight line due to the triaxial halo, without the flattened disk. Dashed line shows the contribution of the disk alone, in the case of a spherical halo. At large distances from the center, most of the deflection is due to the asphericity of the halo. As a check of numerical accuracy, dotted line shows that in a spherical bulge+halo potential without the disk, the inferred angle is close to zero as expected.

which leads to large apparent variations of the transverse velocity. At larger distances, a significant part of v_{tr} represents the reflex motion of the Sun around the Galactic center.

For this and subsequent figures, we have chosen a fiducial triaxial halo model with the axis ratios $q_1/q_3 = 0.9$, $q_2/q_3 = 0.7$, and the major axis aligned with the Z-coordinate. Our choice is motivated by the orientation of satellite galaxies and their counterparts in cosmological simulations (e.g., Zentner et al. 2005; Libeskind et al. 2005), which indicates that the dark matter halo may be prolate and oriented perpendicular to the plane of the disk. The prolate Galactic halo based on the kinematics of the Sagittarius dwarf debris has been claimed by Helmi (2004b) but disputed by Johnston et al. (2005). Even the evidence based on the satellites is inconclusive at present (c.f., Navarro et al. 2004; Bailin et al. 2005) and our fiducial model should be considered as an example only.

Figure 2 shows the deviation of the orbit from a straight line, as measured by the angle between the radius vector and the velocity vector in the Galactocentric frame. Owing to the very large ejection velocity from the center, this deviation is always small, $\lesssim 1\%$. Therefore, the expected transverse velocities should be of the order 1% of the total velocity, or several km s^{-1} .

Figure 2 also shows that the asymmetry of the potential due to the flattened disk causes a smaller deflection than that due to the triaxial halo, for stars at large dis-

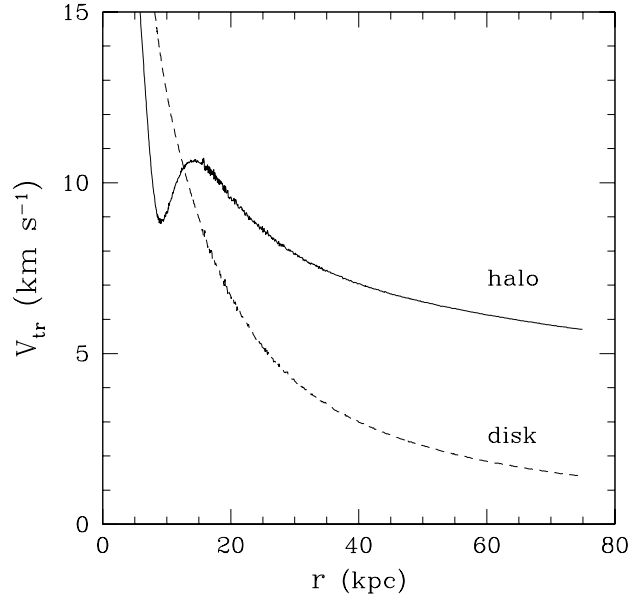


FIG. 3.— Difference between the velocities perpendicular to the line of sight (solid line) for the orbits in the triaxial and spherical halos shown on Fig. 1. For comparison, dashed line shows the difference between the transverse velocities in the cases of a spherical halo with and without the flattened disk. These differences in v_{tr} lead to the differences in the expected proper motions of the HVS for different shapes of the Galactic halo.

tances. In the case of a spherical halo, the deflection contributed by the disk peaks at $r \approx 10$ kpc but quickly declines at larger distances where the disk density vanishes and the direction of the orbit aligns with the velocity vector. Because of this geometric effect, the angle θ_{disk} falls inversely proportional to the distance at $r > 40$ kpc. On the other hand, the halo density profile is still close to isothermal at these distances, and the potential quadrupole induced by halo triaxiality, $\delta\Phi \propto \rho_h(r)r^2$, is a weak function of r . This quadrupole causes a continuous deflection of the orbit, $\delta v \sim \delta\Phi/v$. Hence, measuring the deviation of the trajectory of the HVS from a radial direction is sensitive to the halo triaxiality and relatively insensitive to any uncertainties in the mass model of the disk.

A measurement of the proper motion of the HVS would give the transverse velocity in the reference frame associated with Earth (or after appropriate corrections, with the LSR). In addition to the perpendicular component of the Galactocentric velocity \mathbf{v} , the measured velocity would include the transverse component of the Solar motion around the Galaxy, \mathbf{v}_{\odot} , as well as a correction due to the Earth being at a distance $R_{\odot} = 8$ kpc from the Galactic center. At large distances, $d \gg R_{\odot}$, where the angle $\theta \ll 1$, the observed transverse velocity is

$$\mathbf{v}_{tr,obs} \approx v\boldsymbol{\theta} + v\frac{\mathbf{R}_{\odot} \times \hat{\mathbf{e}}_{\perp}}{d} + \mathbf{v}_{tr\odot}, \quad (8)$$

where $\boldsymbol{\theta}$ is the vector of length θ perpendicular to the line of sight, \mathbf{R}_{\odot} is the vector of length R_{\odot} towards the Galactic center, and $\hat{\mathbf{e}}_{\perp}$ is the unit vector perpendicular to both \mathbf{R}_{\odot} and the line of sight. The last two compo-

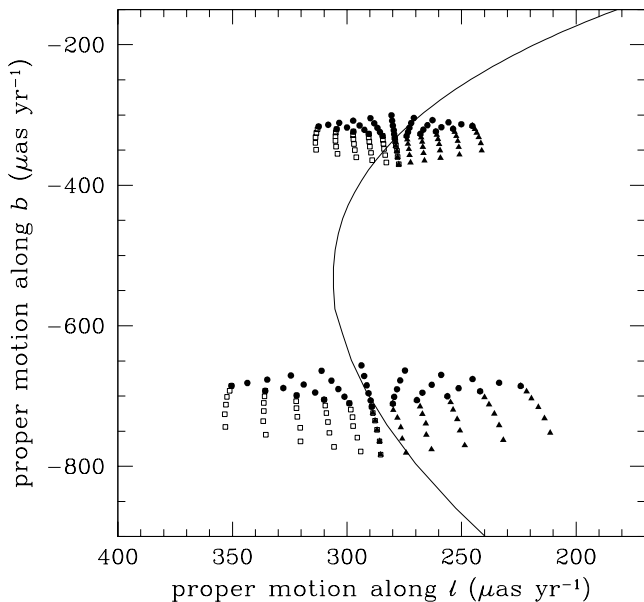


FIG. 4.— Expected proper motions of the HVS under a range of different assumptions about the shape and orientation of the Galactic dark matter halo. The two components of the proper motion are in the directions of increasing Galactic coordinates, l and b . The family of models with the halo major axis along the Galactic X-coordinate is shown by triangles, along Y-coordinate by open squares, and along Z-coordinate by filled circles. The upper and lower groups of the proper motions are for two assumed distances of the HVS of 70 kpc and 40 kpc, respectively. The solid line shows the predicted proper motions for a HVS distance from Earth varying from 30 (bottom) to 140 kpc (top), assuming a spherical dark matter halo.

nents depend only on the distance and angular coordinates of the HVS but not on the shape of the halo and the disk. For a given position of the HVS, the differences in the expected proper motions are only due to the deflections by the halo and the disk.

Figure 3 shows the differences of the velocities perpendicular to the line-of-sight for the triaxial and spherical halos. For the chosen halo model, $\Delta v_{tr} \approx 6 \text{ km s}^{-1}$. This velocity difference is again dominated by the triaxiality of the halo, as is the case with the deflection angles. At $r > 10 \text{ kpc}$, the contribution of the flattened disk decreases as $\Delta v_{tr,disk} \propto d^{-1}$. The halo contribution also decreases at large radii but only because of the smaller projection of the Solar reflex motion along the orbit (third term in eq. [8]). By construction of the orbits that reproduce the observed positions of the HVS, at its current distance Δv_{tr} is independent of the solar motion.

3. RECONSTRUCTION OF THE HALO SHAPE

Placing constraints on the shape and orientation of the Galactic halo is important for testing current models of galaxy formation. Current ground-based measurements of the proper motion of the HVS are inconclusive and consistent with zero within large uncertainties (see Brown et al. 2005). However, the exquisite resolution of the *Hubble Space Telescope* (*HST*) would allow one to

measure the proper motion of the HVS, or place useful limits on its value, within just a few years.

The predicted proper motions in Galactic angular coordinates are plotted in Figure 4. The velocity transverse to the line of sight is projected on two axes in the directions of increasing Galactic coordinates l and b . The two groups of points represent sets of triaxial halo models at two discrete distances, while the solid curve represents a spherical model at a continuum of distances. The absolute values of the proper motions vary from $400 \mu\text{as yr}^{-1}$ to $900 \mu\text{as yr}^{-1}$, depending on which distance is chosen for the HVS (70 and 40 kpc, respectively).

Note that the loci of the two distributions of the proper motions for two assumed distances are well separated from each other, and therefore the true distance of the HVS can be cleanly determined from a proper-motion measurement accurate to $\sigma_\mu \sim 100 \mu\text{as yr}^{-1}$.

With an accuracy of $\sigma_\mu \sim 20 \mu\text{as yr}^{-1}$ we can place interesting constraints on the orientation of the Galactic halo. In particular, if the major axis of the halo is aligned with the direction to the Galactic center ($l = 0$), the predicted components μ_l all lie below $\mu_l < 280 \mu\text{as yr}^{-1}$. If the major axis is in the direction of solar rotation, $\mu_l > 300 \mu\text{as yr}^{-1}$. If the halo is prolate with the major axis aligned with the disk rotation axis, then the predicted μ_b component of the proper motion is well constrained to be either -320 ± 20 or $-700 \pm 40 \mu\text{as yr}^{-1}$, for the assumed distances of 70 and 40 kpc, respectively. These estimates are valid under our assumption that the halo axes are aligned with the Galactic coordinate axes, i.e., X along $l = 0$, Y along $l = 90^\circ$, and Z perpendicular to the disk plane.

With an accuracy of $\sigma_\mu = 10 \mu\text{as yr}^{-1}$ we can attempt a reconstruction of the halo axis ratios. Figure 5 shows an example of such a future reconstruction given a hypothetical measurement of the proper motions of the HVS, μ_l^{obs} and μ_b^{obs} . The three sets of models (each with the major axis aligned with one of the coordinate axes) are combined in a single plot of the axis ratios $q_2/q_1 = Y/X$ versus $q_3/q_1 = Z/X$. The lower left part of the plot corresponds to the case of the major axis along the Galactic X-coordinate ($q_1 = 1$), whereas the lower right and upper left parts correspond to the major axis along the Y-coordinate ($q_2 = 1$) and the Z-coordinate ($q_3 = 1$), respectively. In this plot we calculate

$$\chi^2 = \frac{(\mu_l - \mu_l^{\text{obs}})^2 + (\mu_b - \mu_b^{\text{obs}})^2}{\sigma_\mu^2} + \frac{(d - d_{\text{obs}})^2}{\sigma_d^2} \quad (9)$$

assuming that the true distance of the HVS is unknown ($\sigma_d \rightarrow \infty$) and search for all predicted proper motions μ_l, μ_b at all possible distances between 20 kpc and 100 kpc that minimize χ^2 . The assumed observed proper motions, however, correspond to the fiducial model with $q_1/q_3 = 0.9$, $q_2/q_3 = 0.7$, and the distance of 70 kpc.

According to Figure 5, a certain range of the axis ratios can be excluded based on the proper motion accuracy of $\sigma_\mu = 10 \mu\text{as yr}^{-1}$. However, there are strong triaxiality-distance degeneracies. The best-fitting axis ratios form a band stretching across the diagram because different halo shapes with a somewhat different target distance can produce similar proper motions. This effect is evident in Figure 4. The inferred distances for our fiducial model range from 67 to 78 kpc. The allowed contours would be reduced if the actual distance of the HVS were

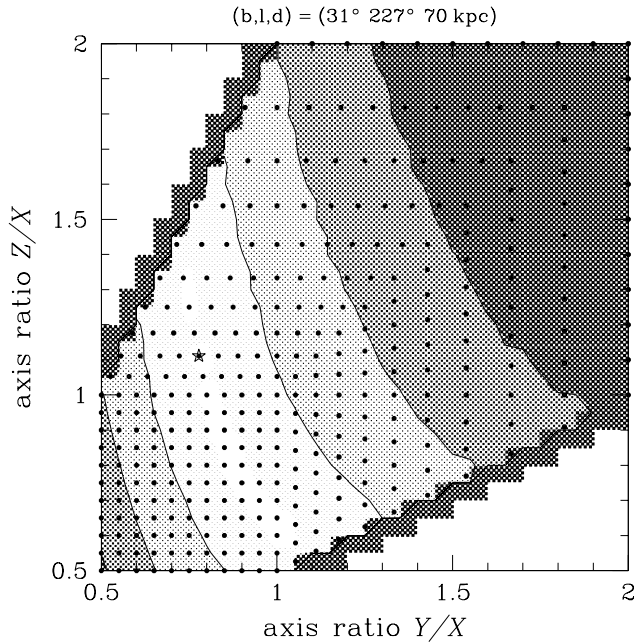


FIG. 5.— Reconstruction of the halo shape from the (assumed) measured proper motions of the HVS. All calculated triaxial models are marked by filled dots corresponding to their axis ratios. Lines represent 1σ , 2σ , and 3σ contours, assuming measurement errors of $10\mu\text{as yr}^{-1}$. The assumed proper motions correspond to the triaxial model with the axis ratios $q_1/q_3 = 0.9$, $q_2/q_3 = 0.7$, which are marked by a star, and the distance of the HVS of $d = 70$ kpc.

known, but it needs to be measured to better than 10% to make a significant difference. Also, if the true distance of the HVS is smaller than the 70 kpc assumed in our fiducial model, the constraints become tighter.

4. TWO, THREE, ... MANY HYPER VELOCITY STARS

4.1. Two Hyper Velocity Stars

Measurements of the proper motions of the single known HVS would already provide interesting constraints on the shape and orientation of the Galactic halo. Yet, the allowed range of axis ratios is fairly broad, even when the measurement errors are as small as $10\mu\text{as yr}^{-1}$. The constraints could become tighter if another HVS were discovered.

For example, suppose that another hypervelocity star, HVS2, were discovered at the same angle $b_2 = 31^\circ$ above the Galactic plane but offset by 45° in longitude, $l_2 = l - 45^\circ = 182^\circ$, and at a hypothetical distance of 50 kpc. Figure 6 shows the superposition of the contours of the original HVS and the new HVS2. The χ^2 contours for the two stars intersect almost perpendicularly to each other and significantly reduce the acceptable range of halo shapes. At the 1σ level the axis ratios would be constrained to better than 20%.

Do all directions of the HVS2 on the sky provide equally useful constraints on the halo axis ratios? Figure 7 shows the contours for the HVS2 offset by 180° in longitude ($l_2 = 47^\circ$) and 30° in latitude ($b_2 = 61^\circ$). These contours also intersect the contours for the original HVS and the resulting constraints are also tight. However, in the case (not shown) that the two stars were at the

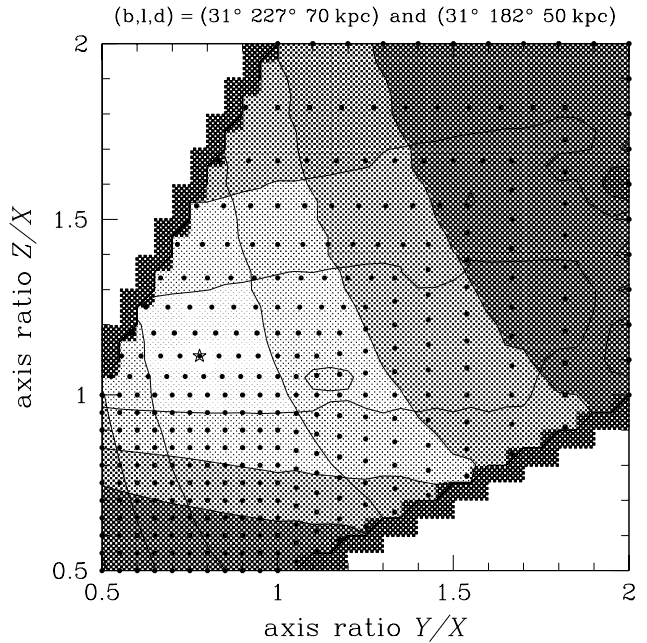


FIG. 6.— Combined reconstructed contours for two HVS, assuming another star were detected at a 45° offset in the Galactic l coordinate, at a distance of 50 kpc from Earth.

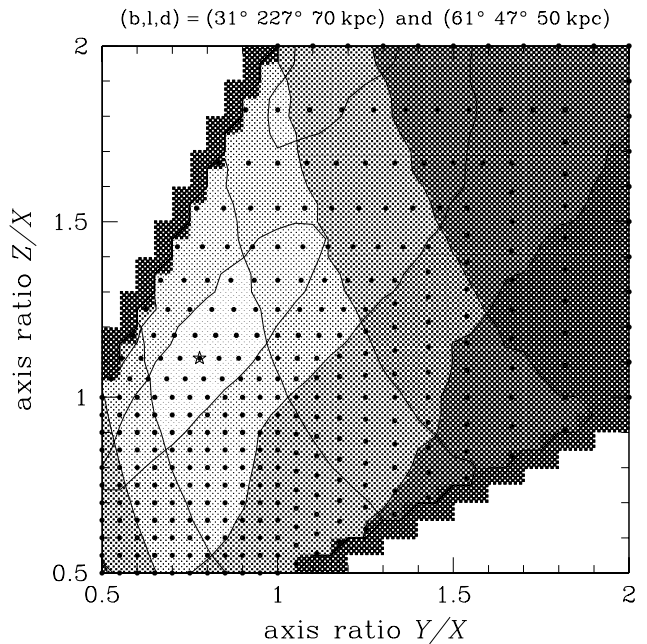


FIG. 7.— Same as Fig. 6, but assuming an offset of 180° in l and 30° in b .

same longitude ($l_2 = 227^\circ$) but only offset in latitude ($b_2 = 61^\circ$), the contours of the HVS2 are almost parallel to those of the HVS and provide no new information. Thus, searching prospective HVSs at different longitudes than the original HVS would yield the most interesting new constraints.

4.2. Three or more Hyper Velocity Stars

Although there are physical motivations (albeit not conclusive) for the halo to be prolate with its major axis perpendicular to the plane of the Galactic disk (e.g. Helmi 2004a; Zentner et al. 2005), the orientation of the other two axes in the plane of the disk is somewhat arbitrary. There is nothing special about the current location of the Sun, which defines the Galactic X -coordinate. Therefore, the halo axes in the plane can be rotated with respect to the Galactic coordinates by any angle between 0 and 90° . This means that even under the most optimistic assumptions, a minimum of three HVSs are required to fix the Galactic potential.

To illustrate the role of three HVSs, we have calculated another set of models, keeping fixed the ratio $q_1/q_3 = 0.9$ and varying two parameters: the ratio q_2/q_3 between 0.5 and 0.9 , and the angle ϕ between the halo axis q_1 and the Galactic X -coordinate between 5° and 90° . Figure 8 shows the resulting contours for a fiducial model in which the q_1 axis is rotated by 60° . The rotation angle is constrained very well, within $5^\circ - 10^\circ$, even if we assume larger measurement errors, $\sigma_\mu = 30 \mu\text{as yr}^{-1}$.

We have also explored the configuration (not shown) in which the halo is oblate rather than prolate, with the minor axis along the rotation axis of the disk. In this configuration the angular momentum vectors of the halo and the disk are parallel to each other, as has often been assumed in the literature. We find that the contours in this model are qualitatively similar to those in Fig. 8, and in particular, angle ϕ can be constrained with a similar accuracy.

If five HVSs were detectable, it would be possible to measure all five parameters of a more general triaxial halo. These would be the two axis ratios, and the three direction angles. Additional HVSs (beyond five) could be used either to improve the precision of the estimates of the first five parameters or to explore halo models of additional complexity.

5. DISCUSSION

We have shown that proper motion measurements of the recently discovered HVS, accurate to $\sigma_\mu \sim 10 \mu\text{as yr}^{-1}$, would place significant constraints on the axis ratios and orientation of the Galactic halo. With only one HVS, such constraints are limited by the triaxiality-distance degeneracies. They can be improved only when the distance is determined to within a few kpc. However, the discoveries and proper motion measurements of several additional HVSs could simultaneously resolve the distance degeneracies of all such stars and produce tighter limits on the triaxiality of the Galactic halo. We now discuss implications of the discovery of multiple HVSs and potential methods of finding more HVSs in future surveys.

5.1. History of Ejection from the Galactic Center

If several hyper velocity stars are found, it may be possible to reconstruct the history of their ejections from the Galactic center and therefore, constrain the rate of binary disruption near the massive black hole. Yu & Tremaine (2003) estimate the rate of ejection from the breakup of binary stars of $\sim 10^{-5} \text{ yr}^{-1}$. If there is another massive black hole in the close vicinity of the

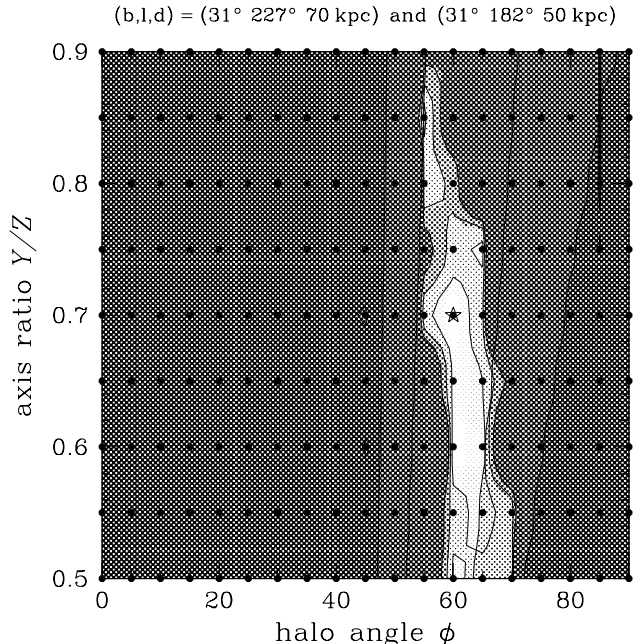


FIG. 8.— Same as Fig. 6, but as a function of angle between the halo axis q_1 and the Galactic X -coordinate. The axis ratio $q_1/q_3 = 0.9$ is kept fixed in this plot. Assumed measurement errors are $30 \mu\text{as yr}^{-1}$.

central black hole at the Galactic center, then stars can be ejected by three-body interactions with the binary system formed by the two black holes. Yu & Tremaine (2003) estimate that the rate of such events $\lesssim 10^{-4} \text{ yr}^{-1}$. The density of the HVSs in the halo can be calculated if HVSs are ejected from the Galactic center isotropically at a steady rate $\dot{N} = 10^{-5} \dot{N}_5 \text{ yr}^{-1}$. The expected number density in this case is $n(r) \approx \dot{N}_5 r^{-2} \text{ kpc}^{-3}$, where r is in kpc.

There are several circumstances that could lead to clumping of HVS ejections in time, e.g., if bursts of star formation (lasting $\sim 1 \text{ Myr}$) or infall of clusters containing intermediate-mass black holes (e.g., Hansen & Milosavljević 2003) led to a rapid increase in the ejection rate. If the global fit to multi-HVS data led to distance estimates accurate to 5 kpc , it would enable one to date individual ejections with an accuracy of about 5 Myr , and therefore, to test whether the ejections were clumped in time.

5.2. How to find HVS?

There are basically two potential methods to find more HVSs: proper motions and radial velocities. For practical reasons, these methods probe two different volumes, the ($\sim 10 \text{ kpc}$) “solar neighborhood” and the outer Galaxy, respectively.

If a star ejected from the Galactic center is passing within $\sim 10 \text{ kpc}$ of the Sun with a speed significantly greater than the escape speed, then its proper motion will be of order $\mu \sim 1000 \text{ km s}^{-1}/10 \text{ kpc} \sim 20 \text{ mas yr}^{-1}$. Given a proper motion survey with precision $\sim 4 \text{ mas yr}^{-1}$, this would be detectable at the 5σ level. Such precision is already available for the sev-

eral thousand square degrees covered by the Sloan Digital Sky Survey (Gould & Kollmeier 2004; Munn et al. 2004). However, robust identification of high-velocity candidates requires not just reliable proper motions, but reliable distances as well. While horizontal branch (HB) stars are approximately standard candles whose distances can be reliably estimated from their colors and magnitudes, halo blue stragglers (BS) can masquerade as HB stars. A BS that was 2 mag dimmer than a HB star would have the same proper motion as a HB HVS but would actually be travelling 2.5 times slower. That is, an ordinary halo BS could easily be misinterpreted as a HB HVS. Similarly, because subdwarfs are often 2 mag dimmer than main-sequence stars of the same color, ordinary subdwarfs could be mistaken for HVS main-sequence stars. To some extent, HVS candidates can be singled out because their trajectories “point back” to the Galactic center. However, since halo stars tend to be on radial orbits, this characteristic is not so distinguishing unless the proper motions are fairly precise.

The situation will change radically when GAIA data become available, not only because of its 4π sky coverage but also because it will provide parallaxes as well as proper motions. At present, these are expected to be $\sigma_\pi \sim 20 \mu\text{as}$ at $V = 15.5$, implying roughly 20% parallax errors for HB stars at 10 kpc. Dimmer stars would be similarly measurable but only within a much smaller volume.

The proper-motion technique does not work at all for HVS stars like SDSS J090745.0+024507 that have already left the Galaxy. The transverse velocities of these stars in the Galactic frame are only $v_{tr} \sim v(R_\odot/d)$, where v is their actual velocity and d is their distance (see eq. [8]). This is similar to the value for halo stars, making them not easily distinguishable. Rather, these distant HVS can be reliably identified using radial-velocity surveys of distant stars (as was done for SDSS

J090745.0+024507). The only drawback is that many stars with large photometric distances must be measured to find a small number of HVSs. Since the number density of HVS falls as r^{-2} , while the density of contaminating Galactic stars falls as $r^{-3.5}$, the contamination rate falls for more distant samples. However, more distant stars require longer integration times. Moreover, once found, they require more accurate proper motions (on fainter stars!) to derive the same precision on the transverse velocity, and so to extract similar information about the Galactic potential. Thus, there do not appear to be any easy paths to finding HVSs.

Finally, we remark that the simulations we have conducted have assumed proper-motion errors of $\sigma_\mu \sim 10 - 50 \mu\text{as yr}^{-1}$, the upper end of which is roughly what is achievable using the *HST* Advanced Camera for Surveys with a 4-year baseline. It is open to question whether *HST* will even be operational in 4 years, let alone in the additional time required to first find the HVSs. Over the longer term, the *Space Interferometry Mission (SIM PlanetQuest)* expects to achieve $\sigma_\mu \sim 4 \mu\text{as yr}^{-1}$ for targeted stars with $V \lesssim 20$. For stars toward this faint limit, this very high precision can be achieved only by quite long integrations, typically several tens of hours. However, the integration time falls inversely as the square of the desired precision, so that exposure times could be fine-tuned to the precision required for each specific HVS.

We acknowledge discussions at the OSU Astro Coffee that initiated this project. OYG acknowledges support from NASA ATP grant NNG04GK68G. Work by AG is supported by grant AST 02-01266 from the NSF and by JPL contract 1226901. ARZ is supported by the Kavli Institute for Cosmological Physics at The University of Chicago and the NSF under grant PHY 0114422.

REFERENCES

- Bailin, J., Kawata, D., Gibson, B. K., Steinmetz, M., Navarro, J. F., Brook, C. B., Gill, S. P. D., Ibata, R. A., Knebe, A., Lewis, G. F., & Okamoto, T. 2005, *ApJ*, 627, L17
- Binney, J. & Tremaine, S. 1987, *Galactic dynamics* (Princeton, NJ, Princeton University Press, 1987, 747 p.)
- Blumenthal, G. R., Faber, S. M., Flores, R., & Primack, J. R. 1986, *ApJ*, 301, 27
- Brown, W. R., Geller, M. J., Kenyon, S. J., & Kurtz, M. J. 2005, *ApJ*, 622, L33
- Bullock, J. S. 2002, in *Proceedings of the Yale Cosmology Workshop “The Shapes of Galaxies and Their Dark Matter Halos”*, (28-30 May, 2001). P.Natarajan (ed.). Singapore: World Scientific, 109
- Dehnen, W. & Binney, J. J. 1998, *MNRAS*, 298, 387
- Gnedin, O. Y., Kravtsov, A. V., Klypin, A. A., & Nagai, D. 2004, *ApJ*, 616, 16
- Gould, A. & Kollmeier, J. A. 2004, *ApJS*, 152, 103
- Hansen, B. M. S. & Milosavljević, M. 2003, *ApJ*, 593, L77
- Helmi, A. 2004a, *MNRAS*, 351, 643
- , 2004b, *ApJ*, 610, L97
- Hernquist, L. 1990, *ApJ*, 356, 359
- Hills, J. G. 1988, *Nature*, 331, 687
- Ibata, R., Lewis, G. F., Irwin, M., Totten, E., & Quinn, T. 2001, *ApJ*, 551, 294
- Jing, Y. P. & Suto, Y. 2002, *ApJ*, 574, 538
- Johnston, K. V., Law, D. R., & Majewski, S. R. 2005, *ApJ*, 619, 800
- Kazantzidis, S., Kravtsov, A. V., Zentner, A. R., Allgood, B., Nagai, D., & Moore, B. 2004, *ApJ*, 611, L73
- Klypin, A., Zhao, H., & Somerville, R. S. 2002, *ApJ*, 573, 597
- Libeskind, N. I., Frenk, C. S., Cole, S., Helly, J. C., Jenkins, A., Navarro, J. F., & Power, C. 2005, *MNRAS*, submitted; astro-ph/0503400
- Majewski, S. R., Skrutskie, M. F., Weinberg, M. D., & Ostheimer, J. C. 2003, *ApJ*, 599, 1082
- Miyamoto, M. & Nagai, R. 1975, *PASJ*, 27, 533
- Munn, J. A., Monet, D. G., Levine, S. E., Canzian, B., Pier, J. R., Harris, H. C., Lupton, R. H., Ivezić, Ž., Hindsley, R. B., Hennessy, G. S., Schneider, D. P., & Brinkmann, J. 2004, *AJ*, 127, 3034
- Navarro, J. F., Abadi, M. G., & Steinmetz, M. 2004, *ApJ*, 613, L41
- Navarro, J. F., Frenk, C. S., & White, S. D. M. 1997, *ApJ*, 490, 493
- Ryden, B. S. & Gunn, J. E. 1987, *ApJ*, 318, 15
- Yu, Q. & Tremaine, S. 2003, *ApJ*, 599, 1129
- Zentner, A. R., Kravtsov, A. V., Gnedin, O. Y., & Klypin, A. A. 2005, *ApJ*, in press; astro-ph/0502496